

Peaks separation of the nonlinear refraction and nonlinear absorption induced by external electric field

Dongyi Guan, Zhenghao Chen, Yueliang Zhou, Kui-Juan Jin, and Guozhen Yang^{a)}

Beijing National Laboratory for Condensed Matter Physics, Institute of Physics, Chinese Academy of Science, P.O. Box 603, Beijing 100080, China

(Received 9 November 2005; accepted 25 January 2006; published online 16 March 2006)

To investigate the relation between the nonlinear susceptibility and the wavelength, Ag:BaTiO₃ composite films were synthesized on MgO(100) substrates under different external electric fields using pulsed laser deposition. The nonlinear optical properties of the films were measured by *z*-scan in the wavelength of 355–650 nm. It is found that with increasing the electric field, the peak of the nonlinear refraction index shifts to longer wavelength (redshift) and is separated from the peak of the nonlinear absorption. With the separation, the values of $|\text{Re } \chi^{(3)}/\text{Im } \chi^{(3)}|$ can be enhanced obviously. © 2006 American Institute of Physics. [DOI: 10.1063/1.2186518]

Many composite films that have metal particles embedded in dielectric hosts are broadly researched due to their potential applications.^{1–3} The metal composite films are less practical at present because the surface-plasmon resonance, which not only enhances the optical nonlinearity, but also enhances the absorption of the films. Many methods are used to reduce the absorption in recent years.^{4,5} It is pointed out in theory that the geometric anisotropy of a suspension of metal nanocrystals in a dielectric host could separate the absorption peak from the nonlinearity enhancement peak.^{6,7} In this letter, we fabricate the composite films under an external electric field and measure the third-order nonlinear susceptibility in the wavelength range of 355–650 nm using the *z*-scan technique, and find that the nonlinear absorption peak are separated from the nonlinear refraction peak. The results indicate that the $|\text{Re } \chi^{(3)}/\text{Im } \chi^{(3)}|$ can be enhanced by 3–4 times due to the applying of external electric field.

In order to describe the optical property of the composite films, we invoke the effective medium approximation (EMA) for anisotropic media. The local constitutive relation is given by $\mathbf{D}=(\epsilon+\chi|\mathbf{E}|^2)\mathbf{E}$, where ϵ is the dielectric constant and χ is the third-order Kerr nonlinear susceptibility. We assign two different occupation probabilities parallel (p_{\parallel}) and perpendicular (p_{\perp}) to a particular direction, i.e., uniaxial anisotropy. A value r , the ratio of p_{\perp} to p_{\parallel} , is used to characterize the anisotropy in the film. The film is isotropic when $r=1$; and with r decreasing to 0, the anisotropy in the film becomes more and more distinct. The coupled EMA self-consistency equations read⁶

$$p_{\parallel} \frac{\epsilon_1 - \epsilon_{\parallel}}{\epsilon_1 + z_{\parallel} \epsilon_{\parallel}} + (1 - p_{\parallel}) \frac{\epsilon_2 - \epsilon_{\parallel}}{\epsilon_2 + z_{\parallel} \epsilon_{\parallel}} = 0, \quad (1)$$

$$p_{\perp} \frac{\epsilon_1 - \epsilon_{\perp}}{\epsilon_1 + z_{\perp} \epsilon_{\perp}} + (1 - p_{\perp}) \frac{\epsilon_2 - \epsilon_{\perp}}{\epsilon_2 + z_{\perp} \epsilon_{\perp}} = 0, \quad (2)$$

where z_{\parallel} and z_{\perp} are the parameters parallel and perpendicular to the applied dc field, ϵ_1 and ϵ_2 are the constituent dielectric functions, and ϵ_{\parallel} and ϵ_{\perp} are the effective dielectric functions parallel and perpendicular to the applied dc field. We limit

the situation to two dimensions (2D) due to the films are very thin. In 2D, the z parameters are given by⁶

$$z_{\parallel} = \frac{\tan^{-1} \sqrt{\epsilon_{\perp}/\epsilon_{\parallel}}}{\tan^{-1} \sqrt{\epsilon_{\parallel}/\epsilon_{\perp}}}, \quad (3)$$

$$z_{\perp} = \frac{\tan^{-1} \sqrt{\epsilon_{\parallel}/\epsilon_{\perp}}}{\tan^{-1} \sqrt{\epsilon_{\perp}/\epsilon_{\parallel}}}.$$

Since we are interested in the optical response parallel to the polarization direction of the laser used in *z*-scan measurements, we can let $p=p_{\parallel}$ and $\epsilon_e=\epsilon_{\parallel}$. Calculations have indicated that the peaks of absorption and nonlinear susceptibility will both shift when the film has some anisotropy. For instance, if the metal particles in the film are prolate spheroid and distributed with some gradation profile, the peaks of absorption and nonlinear susceptibility will shift to long wavelength.⁸

In this study, nanoscale Ag particles embedded in BaTiO₃ thin films (Ag:BaTiO₃) were prepared using a pulsed laser deposition (PLD) technique.⁹ Two Ag chips

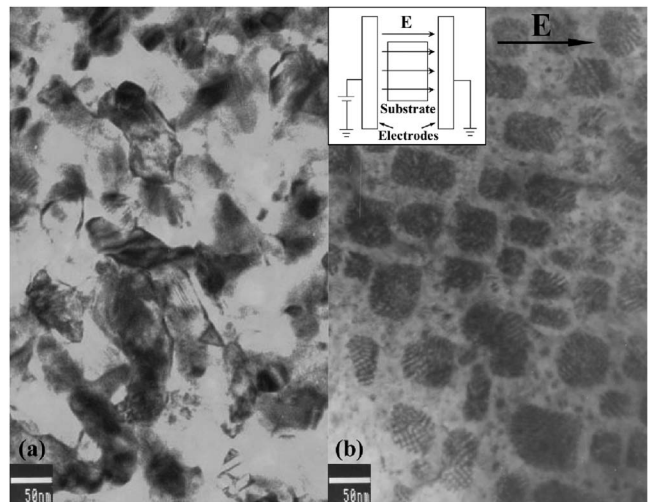


FIG. 1. The TEM images of the Ag:BaTiO₃ composite films. (a) is for the sample a (without applied electric field) and (b) is for the sample b (with an applied electric field of 1000 V/cm). The electric provider is sketched in the inset of (b).

^{a)} Author to whom correspondence should be addressed; electronic mail: yanggz@aphy.iphy.ac.cn

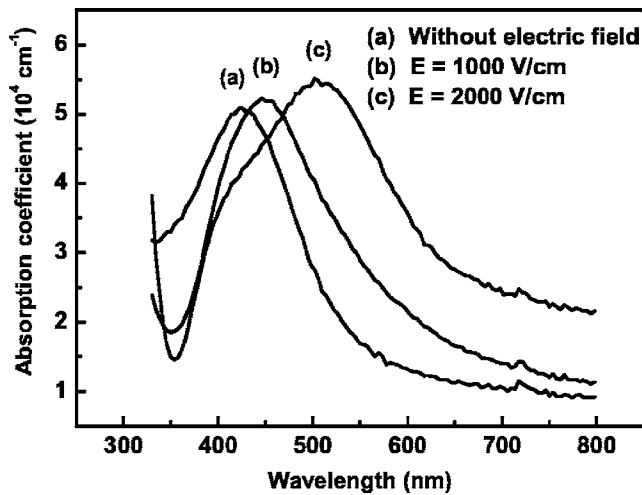


FIG. 2. The optical absorption properties of the films deposited under different electric fields: (a) without electric field; (b) $E=1000$ V/cm; and (c) $E=2000$ V/cm.

were symmetrically placed on the surface of the BaTiO₃ target, covering 1/8 of the target's surface. The target was mounted on a rotating holder so that the Ag particles can be embedded uniformly into the BaTiO₃ hosts. In the PLD processing, a XeCl excimer laser beam, with a wavelength of 308 nm and energy of 1.5 J/cm², was used as the laser source. The deposition chamber was vacuumed to a base pressure of 5.0×10^{-3} Pa, and then pressurized by introducing N₂ to 7.0 Pa. Three films (named 0, 1, 2) were deposited on single crystal (100)MgO (0.5 mm in thickness) substrates, which is 40 mm from the target, under an external electric field parallel to the surface of the substrate of 0, 1000, and 2000 V/cm, respectively. Two metal electrodes are set on both sides of the substrate to provide electric field, which are sketched in the inset of Fig. 1(b). The thickness of the samples was about 50–60 nm. The atomic concentration of Ag particles can also be calculated to be about 5.3% based on the data from x-ray photoelectron spectroscopy spectra.

The distribution and shape of the Ag particles were analyzed by transmission electron microscope in Fig. 1. The dark regions in the images are Ag particles and the light regions are BaTiO₃, and the arrow in Fig. 1(b) denotes the direction of the electric field. It is observed that the Ag particles in sample a are disordered orientation, but some of the Ag particles in sample b are stretched through a same direction, indicating that Ag particles have some ordering orientation in sample b induced by electric field, but the geometric anisotropy was not too obvious. The reason perhaps is the lower applied electrical field.

Figure 2 displays the optical absorption spectra of the Ag:BaTiO₃ thin films in the range from 300 to 800 nm. The data were automatically corrected by the spectrophotometer

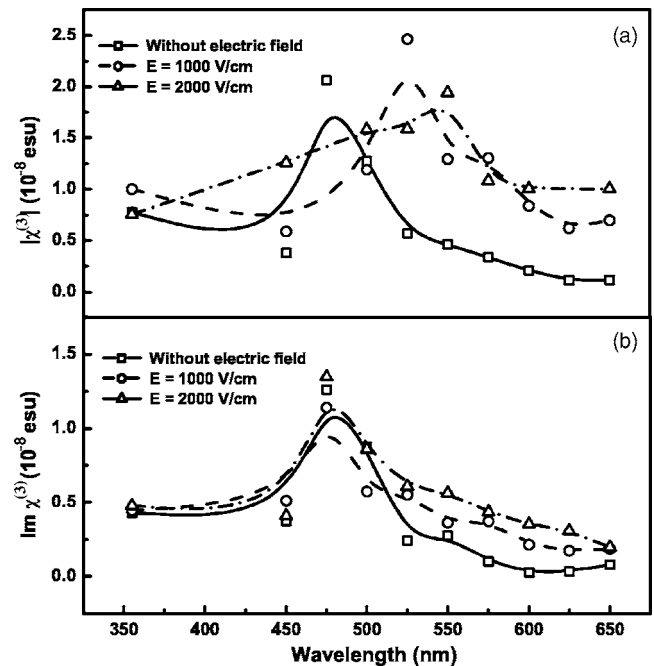


FIG. 3. The relation between the nonlinear susceptibilities and the wavelength. (a) Modulus. (b) Imaginary part.

to account for the absorbance from the MgO substrates. The curves (a)–(c) indicate the absorption peaks as the results of the Ag:BaTiO₃ films deposited under the different external electric fields. Without electric field, the absorption peak due to the surface plasmon resonance of Ag particles is found at the wavelength of 422 nm. When electric fields were applied during the growth of the films, the absorption peaks move to longer wavelengths. With increasing the electric field, the absorption peak shifts to 446 nm at 1000 V/cm and 502 nm at 2000 V/cm. Since the external electric field can change the distribution of Ag particles and make them oriented to its direction, the frequency of the surface plasmon resonance of Ag particles is decreased so that the redshift of the absorption peak occurs. This phenomenon for the orientation of the Ag particles is in good agreement with Sheng's theory.⁶

To find the relation between the third-order nonlinear susceptibility of the films and the wavelength, we measured the nonlinear susceptibility in the wavelength range of 355–650 nm using the z -scan technique. The z -scan measurements were performed using an OPA-704 multiwavelength optical parametric laser with the pulse width of 25 ps. The laser beam was focused on the sample with a 120 mm focal length lens, leading to a measured beam waist of 30 μ m. The pulse energy at the focus is about 8.5 μ J. The Rayleigh length z_R was calculated to be 5.3 mm, which was much longer than the film plus substrate thickness. The transmitted beam energy, the reference beam energy, and their ratios

TABLE I. Linear and nonlinear optical properties near the peak of nonlinear susceptibility of each sample.

Sample	λ (nm)	α (10^4 cm ⁻¹)	$ \chi^{(3)} $ (10^{-8} esu)	$\text{Im } \chi^{(3)}$ (10^{-8} esu)	$ \text{Re } \chi^{(3)} /\text{Im } \chi^{(3)}$	$ \chi^{(3)} /\alpha$ (esu cm)
0	475	3.82	2.07	-1.26	1.30	5.41×10^{-13}
1	525	3.42	2.44	-0.553	4.30	7.16×10^{-13}
2	550	4.84	1.94	-0.564	3.30	4.02×10^{-13}

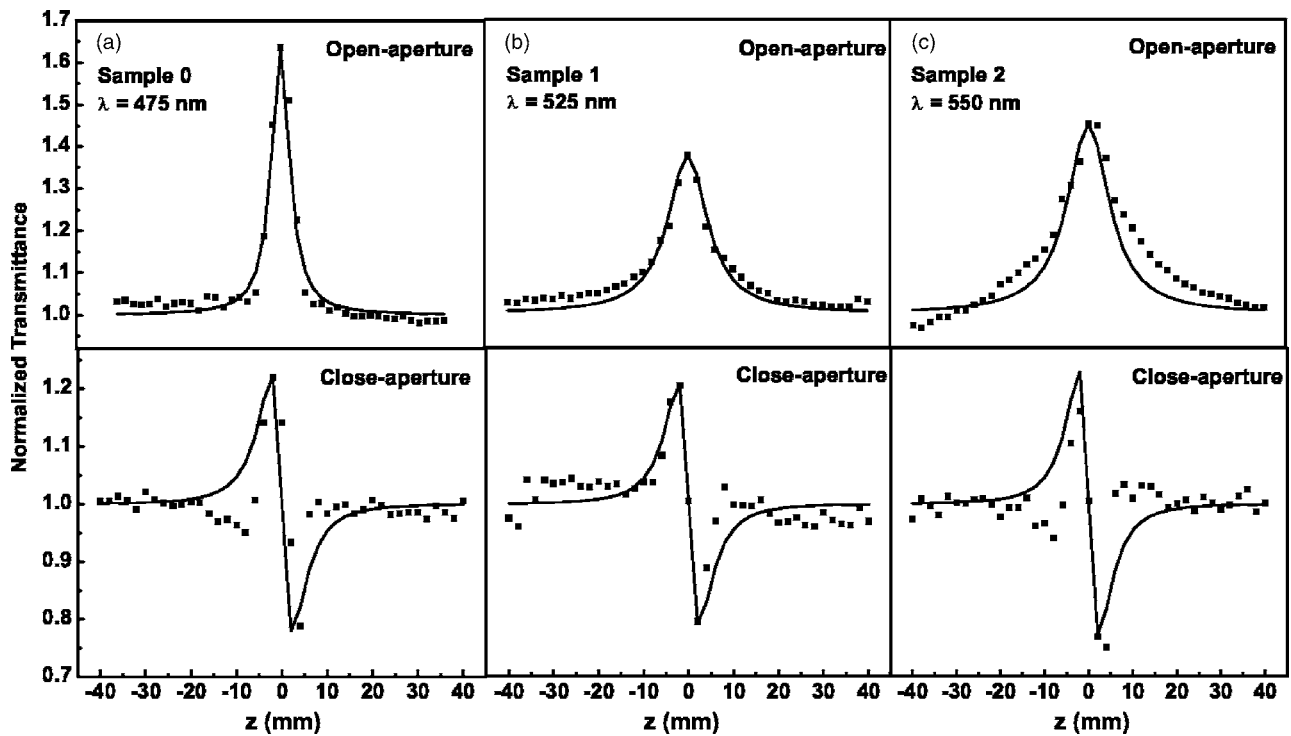


FIG. 4. The z -scan data at the peak of each sample's nonlinear refraction. (a), (b), and (c) denote samples 0, 1, and 2, respectively. The solid lines indicate the theoretical fit.

were measured using an energy ratiometer simultaneously. The data were recorded every 25 nm from 475 to 650 nm, and the data at 355 nm was obtained using a YAG571C-10 laser with the pulse width of 25 ps.

Figure 3 represents the relations between the nonlinear susceptibilities $\chi^{(3)}$ and the wavelength with the films deposited under different electric fields, where (a) and (b) show the modulus and imaginary parts of the nonlinear susceptibilities respectively. It is observed from Fig. 3(a) that the peaks of $|\chi^{(3)}|$ shift to longer wavelengths with increasing the electric field, similar to the peaks of absorption. This result agrees with the calculation.⁸ However, Fig. 3(b) indicates that the peaks of $\text{Im } \chi^{(3)}$ are barely influenced by the external electric field. That means, the maximum of the nonlinear refraction is separated from the nonlinear absorption due to the orientation of the Ag particles, which is induced by the external electric field.

Typical open aperture (OA) and close aperture (CA) z -scan profiles for sample 0, 1, and 2 at their peak of nonlinear refraction each are shown in Figs. 4(a)–4(c), respectively. The solid lines are theoretical fits. Because the MgO substrate in our experiment has a very small nonlinear optical response in visible range, which has been measured by the same method, the high nonlinear optical properties observed here resulted from the films. From the OA and CA curves the nonlinear susceptibilities can be calculated by the z -scan theory described previously.^{10,11} The results are summarized in Table I. Since the nonlinear refraction peak and the absorption peak move to the same direction, the values of $|\chi^{(3)}|/\alpha$ do not vary distinctly. However, the values of

$|\text{Re } \chi^{(3)}/\text{Im } \chi^{(3)}|$ increase greatly induced by the separation of the nonlinear refraction peak and the nonlinear absorption peak.

In summary, we fabricated Ag:BaTiO₃ films using the PLD technique under different external electric fields. The linear optical properties of the films are characterized by optical absorption spectra. We measured the optical nonlinearity of the films in 355–650 nm by the z -scan technique. With increasing the external electric field, the peaks of the linear absorption and nonlinear refraction shift to long wavelength, but the peak of the nonlinear absorption does not shift. The values of $|\text{Re } \chi^{(3)}/\text{Im } \chi^{(3)}|$ are 3–4 times enhanced with the applying of external electric field.

¹Y. Hamanaka, K. Fukuta, A. Nakamura, L. M. Liz-Marzán, and P. Mulvaney, *Appl. Phys. Lett.* **84**, 4938 (2004).

²Y. Takeda, J. Lu, O. A. Plaksin, K. Kono, H. Amekura, and N. Kishimoto, *Thin Solid Films* **464–465**, 483 (2005).

³G. Battaglin, E. Cattaruzza, F. Gonella, R. Polloni, B. F. Scremin, G. Mattei, P. Mazzoldi, and C. Sada, *Appl. Surf. Sci.* **226**, 52 (2004).

⁴W. T. Wang, Z. H. Chen, G. Yang, D. Y. Guan, G. Z. Yang, Y. L. Zhou, and H. B. Lu, *Appl. Phys. Lett.* **83**, 1983 (2003).

⁵H. B. Liao, W. Wen, and G. K. L. Wong, *Appl. Phys. A* **A80**, 861 (2005).

⁶K. P. Yuen, M. F. Law, K. W. Yu, and P. Sheng, *Phys. Rev. E* **56**, 1322 (1997).

⁷L. Gao, J. P. Huang, and K. W. Yu, *Phys. Rev. B* **69**, 075105 (2004).

⁸J. P. Huang and K. W. Yu, *J. Opt. Soc. Am. B* **22**, 1640 (2005).

⁹H. Izumi, K. Ohata, T. Hase, K. Suzuki, T. Morishita, and S. Tanaka, *J. Appl. Phys.* **68**, 6331 (1990).

¹⁰M. Yin, H. P. Li, S. H. Tang, and W. Ji, *Appl. Phys. B* **B70**, 587 (2000).

¹¹W. T. Wang, G. Yang, Z. H. Chen, Y. L. Zhou, and H. B. Lu, *J. Appl. Phys.* **92**, 7242 (2002).